Dear Editors and Conference Organizers,

Thank you for taking the time to review our conference paper. We have read through the reviewer comments and have made all the suggested edits. The details of the edits are listed below.

Sincerely,
Yi Chen
Corresponding Author
DSCC2016-9663

Reviewer 1, Comment 1: *In this paper, the authors build off of fairly recent developments in remote temperature sensing using magnets. Using a least-squares method to decompose the magnetic contribution of nearby magnets in three axes, the authors have demonstrated that it is possible to isolate flux changes in a single magnet, and thus derive the temperature of the magnet. The abstract should not be italicized.*
Response: We have changed the abstract to non-italic.

Reviewer 1, Comment 2: *Error due to slight translation or rotation of the magnets during operation is not quantified. It is stated that a single magnet moving 1mm can result in a measurement error of 50 degrees, but what happens if all magnets move, translate a fraction of a millimeter or rotate a fraction of a radian, all at once? The reviewer recommends that the authors add a few sentences or paragraph addressing this issue.*
Response: We have added a few paragraphs discussing this in the section named, "Experimental Considerations." We have added new equation, Eq. (14), showing how it is possible to calculate the error. We also added a paragraph specifically providing numbers for how you can calculate the measurement error of 50 degrees. We also added the procedure necessary to calculate the error magnitude for any arbitrary rotation and/or translation. The text we added is below:

"Magnetic sensors are commonly used for wireless position tracking [8,11,12] due to the high magnetic field sensitivity to position and rotation. This sensitivity, however, is not desirable for temperature tracking because the temperature coefficient of the particle magnetization is very small, on the order of -0.1%/°C. If the temperature error ΔT_j due to position or rotation error is defined as the difference between the temperature estimated with accurately known positions T_j and the temperature estimated without accurately known positions T_j^*, then the temperature error is $\Delta T_j = T_j - T_j^*$. By using Eqs. (12) and (13), it is clear that the temperature error due to position and rotation error is a function of the change in the magnetic field such that,

$$\Delta T_j = \frac{1}{C_T}[(\mathbf{P}^T\mathbf{P})^{-1}\mathbf{P}^T(\mathbf{P}^* - \mathbf{P})]_j. \qquad (14)$$

Note that the $\mathbf{P}$ matrix is equivalent the calibrated magnetic fields such that $\mathbf{P} = \mathbf{B}-\mathbf{C}$ when $T_j = T_0$ and $\mathbf{P}^*$ represents the matrix for the case when the position are not known or are not properly calibrated. This equation can also be used to assess the effects of any untracked magnetic field disturbances on the temperature estimate, including ferromagnetic, paramagnetic, or electric-field generating components.

For the simple case of a single z oriented magnet and a single sensor that are placed 60 mm apart in the x direction, Eqs. (2)-(4) and Eq. (14) show that an untracked position change of 1 mm in the x direction can result in a magnetic field error of approximately 5% which translates to a temperature error of approximately 50°C. If multiple magnets move unpredictably, translating and/or rotating, then Eqs. (2)-(4) and Eq. (14) can be used to predict the error in the temperatures through estimated changes in the magnetic field. Because the error is a function of the **P** matrix, untracked positioning errors on one magnet may manifest as temperature estimation error for all of the magnets in the system.
Due to the difference in relative sensitivity between position and temperature, accurate temperature tracking requires careful consideration of the experimental arrangement."

Reviewer 2, Comment 1: *This paper presents a method of wireless temperature estimation through the use of multiple magnets. In particular, a least square estimation is used to obtain the temperature estimates based on predefined model. The paper is well written and the contribution is clear. The reviewer has the concern that such method is easily disturbed by the surrounding when metal parts (such as a bearing) or external devices generating magnetic field (such as a DC motor) are present. It is suggested that the authors include a paragraph of discussion on this issue, and possibly place some external metal parts between the magnets and sensors acting as disturbances to show the effectiveness of the method.*
Response: The method is disturbed if there are untracked disturbances (unexpected or unpredictable changes in the magnetic field due to moving objects or changing magnetic fields). If the disturbances are stationary, tracked or caused by materials that do not change the magnetic field (materials with a permeability near 1, such as 304 stainless steel), then they have no effect. As suggested by the reviewer, we have added a section at the end of the paper entitled, "Movement of Metal Components" which describes the field deviation caused by different materials such has copper, aluminum, austenitic stainless steel, martensitic stainless steel, and ferritic stainless steel. This shows how the disturbances would affect the measurement if they were not tracked. The percentage deviations can be combined with Eqn. (14) to determine the temperature error. We also provide a column describing the repeatability of measurements if the metal component was tracked. This column shows that the repeatability is very good and that if you track the material, the method would still work very well. The newly added paragraphs are below.

TABLE 2. THE MAGNETIC FIELD DEVIATION IN THE PRESENCE OF METAL PLATES AND THE MEASUREMENT REPEATABILITY AS A FUNCTION OF MOVEMENT OF THE METAL PLATE ON A STAGE

Material	μ_r Ref. [14]	Field Deviation (%)	Repeatability (G)
Air	1	0.06 ± 0.04	0.10 ± 0.08
Copper	1	0.06 ± 0.05	0.15 ± 0.09
Aluminum 6061	1	0.06 ± 0.04	0.15 ± 0.13
Stainless 304 (Austenitic)	1 to 7	0.50 ± 0.52	0.14 ± 0.12
Stainless 313 (Austenitic)	1 to 7	0.54 ± 0.37	0.11 ± 0.09
Stainless 410 (Martensitic)	95 to 750	34.0 ± 3.48	0.14 ± 0.10
Stainless 430 (Ferritic)	1800	86.6 ± 4.90	0.16 ± 0.10

For these experiments, 1.2 to 1.3 mm thick metal plates are moved back and forth between a z oriented magnet and sensor placed 32 mm apart.

"Conventionally, magnetic particle tracking cannot be done in the presence of ferritic materials or materials which bend the magnetic field. Using the calibration procedures presented in this work, however, it is possible to sense temperature in the presence of metals if these materials are tracked and move in repeatable motions. Table II shows how materials with different permeabilities can affect the magnetic field signal. In these experiments, a z oriented magnet is placed 32 mm from a sensor and the magnetic field is measured. A large 152 x 152 mm metal sheet that is 1.2 to 1.3 mm thick is moved back and forth between the sensor and the magnet. The magnetic field deviation in the z axis near the center of the plate as a percentage of measured field with no metal plate is presented in the third column.

Materials like copper and aluminum have a relative permeability near unity and therefore do not alter the field magnitude at all. Austenitic stainless steels can have a relative permeability near unity or slightly higher, especially if they are cold worked. Since these materials are cut with sheet metal break, the edges of the stainless steel will have a higher relative permeability leading to the slightly larger measured field deviations. Martensitic and ferritic stainless steels will have even higher relative permeabilities and will alter the measured field significantly. These materials also tend to be much less uniform and the relative permeability changes significantly as a function of position and orientation of the metal sheet. In some samples and orientations, the deviation observed in the martensitic material can exceed the deviations measured from the ferritic material. If the movement of these metal components is not tracked, then the field deviations listed in the table represent the magnetic field error that can be expected and Eqs. (2)-(4) and Eq. (14) can be used to calculate the expected temperature error. However, if the motions of these metals are tracked and calibrated accurately, then these errors can be removed from the temperature estimate.

In the last column, the repeatability of the magnetic field measurements is measured as the metal sheets are inserted and withdrawn from the magnet and sensor setup. The metal sheets are attached to a slow stage traversing up to 20 mm in 0.5 mm intervals. Before the sheet was inserted, the maximum distance between the sheet edge and the magnet-to-sensor centerline was 13~mm for each sample. The field near the edges of the metal is measured, instead of near the center, because this creates the greatest change in magnetic field as a function of position. The magnetic field at each position is measured multiple times and the repeatability is reported. Although the ferritic stainless steel causes large deviations in the measured field magnitude, the repeatability of the signal through multiple passes is approximately the same as for all the other materials. Therefore, the magnetic field repeatability is essentially only a function of stage positioning repeatability and inherent sensor electrical noise, and not a function of material permeability. This shows that as long as the movement of the material is repeatable and tracked, the temperature sensing scheme can be applied in the presence of metals, including ferritic metals.

Due to the change in the field magnitude, however, the temperature estimation noise for the configuration with ferritic metals may increase. This is because the temperature estimate, for the example of a single magnet and single sensor axis, is essentially the change in the field due to temperature divided by the magnitude of the field without temperature changes. Therefore, if the magnitude of the field decreases and the noise level (or repeatability) is fixed, then the temperature measurement error must increase. Depending on the configuration, magnetic field contributions from materials with $\mu_r \neq 1$ may not sum linearly with existing magnetic fields. Therefore, sequence number calibrations should be conducted for each permutation of interest for the positions of the $\mu_r \neq 1$ metal and magnets."

Draft Recommendations/Comments: *The Conference Editorial Board has reached a positive decision for your submission. Please pay attention to the reviewers' comments and revise the manuscript accordingly when you prepare the final manuscript. We believe this will help improving the quality of the manuscript. Please also make sure all the formatting details are followed. Please complete the copyright form and submit your final paper by the deadlines specified online.*
We look forward to seeing you in Minneapolis!

Proceedings of the ASME 2016 Dynamic Systems and Control Conference
DSCC2016
October 12-14, 2016, Minneapolis, MN, USA

DSCC2016-9663

WIRELESS TEMPERATURE SENSING USING PERMANENT MAGNETS FOR MULTIPLE POINTS UNDERGOING REPEATABLE MOTIONS

Yi Chen*, Oksana Guba, Carlton F. Brooks, Christine C. Roberts,
Bart G. van Bloemen Waanders, and Martin B. Nemer
Sandia National Laboratory
P.O. Box 5800
Albuquerque, NM 87185, USA
*Email: yichen@sandia.gov

ABSTRACT

Temperature monitoring is essential in automation, mechatronics, robotics and other dynamic systems. Wireless methods which can sense multiple temperatures at the same time without the use of cables or slip-rings can enable many new applications. A novel method utilizing small permanent magnets is presented for wirelessly measuring the temperature of multiple points moving in repeatable motions. The technique utilizes linear least squares inversion to separate the magnetic field contributions of each magnet as it changes temperature. The experimental setup and calibration methods are discussed. Initial experiments show that temperatures from 5 to 50 °C can be accurately tracked for three neodymium iron boron magnets in a stationary configuration and while traversing in arbitrary, repeatable trajectories. This work presents a new sensing capability that can be extended to tracking multiple temperatures inside opaque vessels, on rotating bearings, within batteries, or at the tip of complex end-effectors.

Sandia National Laboratories is a multi-program laboratory managed and operated by Sandia Corporation, a wholly owned subsidiary of Lockheed Martin Corporation, for the U.S. Department of Energy's National Nuclear Security Administration under contract DE-AC04-94AL85000. The United States Government retains and the publisher, by accepting the article for publication, acknowledges that the United States Government retains a non-exclusive, paid-up, irrevocable, world-wide license to publish or reproduce the published form of this manuscript, or allow others to do so, for United States Government purposes.

NOMENCLATURE

$\mathbf{A}$	Temperature solution vector
A_j	Temperature solution magnitude
a	X-position of the magnet
$\mathbf{B}$	Magnetic field vector
B_i	Magnetic field magnitude
B_T	Magnetic field strength
b	Y-position of the magnet
$\mathbf{C}$	Magnetic field offset constant vector
C_i	Magnetic field offset constants
C_T	Temperature coefficient of the magnet
c	Z-position of the magnet
$\mathbf{H}$	Magnet orientation vector
I	Total number of sensors
i	Sensor index
J	Total number of magnets
j	Magnet index
k	Position sequence number
L	Characteristic length of the magnet
M_0	Uniform magnetization
m	X-orientation vector of the magnet
n	Y-orientation vector of the magnet
$\mathbf{P}$	Position, orientation, and calibrated magnetic field matrix
P_{ij}	Position, orientation, and calibrated magnetic field magnitude
p	Z-orientation vector of the magnet
R_{ij}	Radial distance from the sensor to the magnet
T_j	Temperature of the magnet
T_0	Calibration temperature
V	Volume of the magnet
$\mathbf{X}$	Relative location of sensor with respect to the magnet

x X-position of the sensor
$\mathbf{Y}$ Calibrated sensor measurement vector
y Y-position of the sensor
z Z-position of the sensor
μ_0 Permeability of free space
μ_r Relative permeability

INTRODUCTION

Wireless temperature sensing can be an essential tool in dynamic mechatronic systems. In machinery, temperature is often a good indicator for fault conditions as well as operating efficiency. Wireless temperature sensing techniques are useful in rotating or free-moving environments when cables or slip-rings are prohibitive. Applications include monitoring bearing, battery, and machine temperatures when wire feedthroughs are prohibitive and where there is limited optical access [1–3]. In many cases, it is desirable to measure multiple temperature points to create temperature maps, determine heat flows, or to pinpoint the location of hot-spots.

Wireless temperature sensing can be accomplished with a variety of methods including techniques which use externally driven passive inductive behaviors [1], externally driven magnetic behaviors [4], or techniques that use batteries and wireless transmitters. Systems requiring batteries can only operate for a limited amount of time and systems using power electronics for wireless transmission or energy harvesting can be prohibitively large for some applications. Passive inductive and non-permanent magnet systems require the use of an external bias or driving source.

Temperature sensing with permanent magnets presents one alternative that does not require batteries or external biasing sources. Non-reversible Curie temperature behaviors have been exploited for temperature sensing in the literature [5, 6]. The magnetic field strength also changes as a function of temperature in a linear fashion below the Curie temperature. This has been successfully used to sense the temperature of one stationary magnet through bearings and metal vessels [2,3,7]. However, the temperature measurement of several closely spaced magnets to obtain temperature gradient information has not been explored in the literature. The ability to measure multiple closely spaced magnet temperatures wirelessly can enable a large variety of applications from monitoring the temperature of permanent magnet motors, objects on the end of rotating end effectors, or objects in opaque enclosed vessels.

This paper describes a unique method for sensing the temperature of several magnets, as shown in Fig. 1, by using inversion techniques. First, the theory for the magnetic field contribution of multiple magnets is discussed. Next, a solution technique is proposed to solve for the field contribution of each magnet separately. These magnetic field values are then converted to temperature measurements. The custom instrumentation used for the experiments and the characteristics of a single magnet are also discussed. Then, the calibration method and measurements of three stationary magnets are explored. Finally, the results show how the temperature of the magnets moving in a repeatable manner can be obtained.

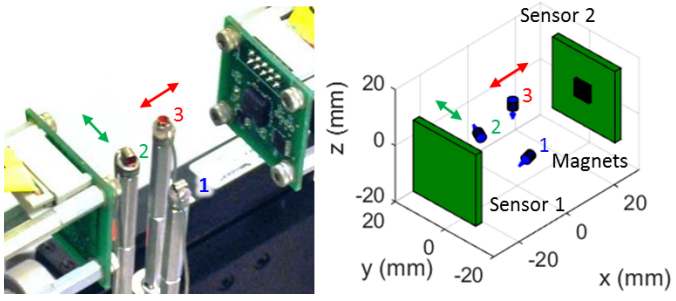

FIGURE 1. WIRELESS, MOVING MAGNET TEMPERATURE SENSING

DISTRIBUTED MAGNET EQUATIONS

The single magnetic dipole equations are discussed here as they serve as a guide for the model developed herein. The magnetic field can be approximated for $i = 1 \ldots I$ three-axis sensors and for $j = 1 \ldots J$ magnetic particles using a dipole model [8]. The magnetic field for a single magnet j at sensor i is,

$$\mathbf{B}_i = B_{Tj}(T_j) \left(\frac{3(\mathbf{H}_j \cdot \mathbf{X}_{ij})\mathbf{X}_{ij}}{R_{ij}^5} - \frac{\mathbf{H}_j}{R_{ij}^3} \right). \quad (1)$$

The magnetic field strength at a temperature T_j can be approximated near room temperature as $B_{Tj}(T_j) \approx \frac{\mu_0}{4\pi}\mu_r M_0 V_j$, where μ_r is the relative permeability of the medium, $\mu_0 = 4\pi \times 10^{-7}$ T·m/A is the magnetic vacuum permeability, $M_0 \approx 1.16 \times 10^6$ A/m is the uniform magnetization of a neodymium iron boron (Nd-Fe-B) magnet near room temperature, and V_j is the magnet volume. The dipole moment magnitude is $M_0 V_j$.

Figure 2 shows the global coordinate system conventions

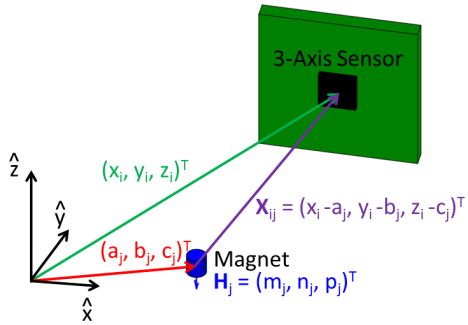

FIGURE 2. THE COORDINATE SYSTEM FOR THE MAGNET AND SENSOR LOCATIONS IS SHOWN.

$$B_{ix} = \sum_{j=1}^{J} B_{Tj}(T_j) \left[\frac{3[m_j(x_i - a_j) + n_j(y_i - b_j) + p_j(z_i - c_j)](x_i - a_j)}{R_{ij}^5} - \frac{m_j}{R_{ij}^3} \right] + C_{ix} \tag{2}$$

$$B_{iy} = \sum_{j=1}^{J} B_{Tj}(T_j) \left[\frac{3[m_j(x_i - a_j) + n_j(y_i - b_j) + p_j(z_i - c_j)](y_i - b_j)}{R_{ij}^5} - \frac{n_j}{R_{ij}^3} \right] + C_{iy} \tag{3}$$

$$B_{iz} = \sum_{j=1}^{J} B_{Tj}(T_j) \left[\frac{3[m_j(x_i - a_j) + n_j(y_i - b_j) + p_j(z_i - c_j)](z_i - c_j)}{R_{ij}^5} - \frac{p_j}{R_{ij}^3} \right] + C_{iz} \tag{4}$$

for the magnets and sensors. The sensor position can be written as $(x_i, y_i, z_i)^T$ and the magnet position can be written as $(a_j, b_j, c_j)^T$. The normalized vector representing the orientation of magnet j is $\mathbf{H}_j = (m_j, n_j, p_j)^T$ such that $m_j^2 + n_j^2 + p_j^2 = 1$. The relative location of the sensor with respect to the magnet is $\mathbf{X}_{ij} = (x_i - a_j, y_i - b_j, z_i - c_j)^T$. The radial distance from the sensor to the magnet can then be calculated as,

$$R_{ij} = \sqrt{(x_i - a_j)^2 + (y_i - b_j)^2 + (z_i - c_j)^2}. \tag{5}$$

Each sensor has three orthogonal field measurements in the x, y, and z directions that are mathematically rotated into the global coordinate system. These three-axis sensors can be used to identify the magnetic field vector by using,

$$\mathbf{B}_i = B_{ix}\hat{\mathbf{x}} + B_{iy}\hat{\mathbf{y}} + B_{iz}\hat{\mathbf{z}}, \tag{6}$$

where the magnetic field components in the x, y, and z directions are B_{ix}, B_{iy} and B_{iz} respectively. Assuming that the contributions of multiple magnets can be summed linearly (since the relative permeability of air is 1.0 and Nd-Fe-B magnets is 1.05), then the equations for the field contribution of a distribution of J magnets on I sensors can be written as Eqs. (2)-(4). The offset constants C_{ix}, C_{iy} and C_{iz} are used to capture the magnetic field offsets from external fields such as the magnetic field of the earth or other nearby fixed magnetic field sources.

The dipole model is only an approximation to the real magnetic field distribution of a magnet and this approximation becomes more accurate if the distance between magnets and the distance from the sensors to the magnets increases. Some researchers [8] have suggested that the approximation becomes useful at $R_{ij}/L > 10$, where L is the characteristic length of the magnet. Several models have been proposed for the true magnetic field of permanent magnets including analytical models, distributed monopole models [9], and neural network models [10]. These can be used to modify the Eqs. (2)-(4) to produce more accurate predictions of the field contributions of magnets at each position. The deviation of a real permanent magnet from the dipole model is one factor that makes simultaneous position and temperature tracking a challenging problem. Therefore, it is important to separate the positioning and orientation information in the measurement from temperature information.

A relationship between the magnetic field and the average temperature of the magnet can be approximated by linearizing the scalar magnitude of the magnetic field emitted by a permanent magnet around a calibration temperature T_0 such that,

$$B_{Tj}(T_j) = B_T(T_0)\left[1 - C_T\left(T_j - T_0\right)\right], \tag{7}$$

where T_j is the temperature of the magnet and C_T is the linear temperature coefficient of the particle magnetization. As will be shown later in the paper, this approximation matches the physical behavior of the magnetic field well.

DISTRIBUTED TEMPERATURE SOLUTION

Solving the complex set of equations represented in Eqs. (2)-(4) for position, rotation, and temperature contributions requires non-linear solution techniques and can introduce large errors due to the large position and rotation sensitivity or due to the solution technique [8]. However, if the positions and orientations are known, then the temperature solution simplifies to a series of linear equations. If the unknown temperature information is separate from the known constants associated with geometry, position and orientation, then Eqs. (2)-(4) can be rewritten as,

$$B_{ix} - C_{ix} = \sum_{j=1}^{J} A_j P_{ijx}(\mathbf{X}_{ij}, \mathbf{H}_j), \tag{8}$$

$$B_{iy} - C_{iy} = \sum_{j=1}^{J} A_j P_{ijy}(\mathbf{X}_{ij}, \mathbf{H}_j), \tag{9}$$

$$B_{iz} - C_{iz} = \sum_{j=1}^{J} A_j P_{ijz}(\mathbf{X}_{ij}, \mathbf{H}_j), \tag{10}$$

where $A_j = 1 - C_T(T_j - T_0)$, and P_{ijx}, P_{ijy}, and P_{ijz} are the functions containing the known positions and orientations of the mag-

nets and sensors multiplied by known magnetic field constant at a calibration temperature $B_T(T_0)$. This can then be reduced to a linear matrix form and written as,

$$\mathbf{Y} = \mathbf{PA}. \tag{11}$$

The variable $\mathbf{Y} = \mathbf{B} - \mathbf{C}$ is a $3I \times 1$ vector representing the calibrated sensor measurements of each axis from the left hand side of Eqs. (8)-(10), $\mathbf{A}$ is the $J \times 1$ vector representing the unknown temperature information, and $\mathbf{P}$ is the $3I \times J$ matrix representing the known particle positions and orientations relative to the sensors multiplied by the magnetization at the calibration temperature $B_T(T_0)$.

If the number of observations is greater than or equal to the number of magnets $3I \geq J$ then matrix inversion, least squares or other minimization techniques can be used to solve for the particle magnetizations,

$$\mathbf{A} = (\mathbf{P}^T\mathbf{P})^{-1}\mathbf{P}^T\mathbf{Y}. \tag{12}$$

Lastly, a temperature solution is obtained for each magnet using,

$$T_j = \frac{1}{C_T}(1 - A_j) + T_0. \tag{13}$$

If the column vectors of $\mathbf{P}$ are linearly dependent, the matrix $\mathbf{P}^T\mathbf{P}$ will not be full rank. There are several situations where magnetic particles can be placed such that $\mathbf{P}^T\mathbf{P}$ contains zero eigenvalues. For example, three magnets oriented in the z direction lying on a line along the y-axis (where $z = 0$ and $x = x_0$) with only a single sensor placed at the origin is not invertible because all the magnets only contribute to the B_z component of the measured magnetic field and all the contributions are linearly dependent.

Several possible practical methods exist for improving the matrix condition number of $\mathbf{P}^T\mathbf{P}$ to enable or improve inversion; the magnetic particles can be moved to different positions, can be rotated into a different orientation or more sensors can be added at different locations in order to change the characteristics of $\mathbf{P}^T\mathbf{P}$. Additional sensors placed near the magnets increases the number of observations and can help reduce variance in the temperature estimates. In general, it is best to simulate a particular magnetic particle distribution and sensor arrangement before conducting an experiment.

Experimental Considerations

Magnetic sensors are commonly used for wireless position tracking [8, 11, 12] due to the high magnetic field sensitivity to position and rotation. This sensitivity, however, is not desirable for temperature tracking because the temperature coefficient of the particle magnetization is very small, on the order of -0.1 %/°C. If the temperature error ΔT_j due to position or rotation error is defined as the difference between the temperature estimated with accurately known positions T_j and the temperature estimated without accurately known positions T_j^*, then the temperature error is $\Delta T_j = T_j - T_j^*$. By using Eqs. (12) and (13), it is clear that the temperature error due to position and rotation error is a function of the change in the magnetic field such that,

$$\Delta T_j = \frac{1}{C_T}[(\mathbf{P}^T\mathbf{P})^{-1}\mathbf{P}^T(\mathbf{P}^* - \mathbf{P})]_j. \tag{14}$$

Note that the $\mathbf{P}$ matrix is equivalent the calibrated magnetic fields such that $\mathbf{P} = \mathbf{B} - \mathbf{C}$ when $T_j = T_0$ and $\mathbf{P}^*$ represents the matrix for the case when the position are not known or are not properly calibrated. This equation can also be used to assess the effects of any untracked magnetic field disturbances on the temperature estimate, including ferromagnetic, paramagnetic, or electric-field generating components.

For the simple case of a single z oriented magnet and a single sensor that are placed 60 mm apart in the x direction, Eqs. (2)-(4) and Eq. (14) show that an untracked position change of 1 mm in the x direction can result in a magnetic field error of approximately 5 % which translates to a temperature error of approximately 50 °C. If multiple magnets move unpredictably, translating and/or rotating, then Eqs. (2)-(4) and Eq. (14) can be used to predict the error in the temperatures through estimated changes in the magnetic field. Because the error is a function of the $\mathbf{P}$ matrix, untracked positioning errors on one magnet may manifest as temperature estimation error for all of the magnets in the system. Due to the difference in relative sensitivity between position and temperature, accurate temperature tracking requires careful consideration of the experimental arrangement.

One possible approach for more accurate temperature estimation is to develop a complex magnetic field distribution model for each magnet to construct the $\mathbf{P}$ matrix. This technique would require knowledge of the position and orientation of the magnets throughout the experiment, either via magnet tracking techniques or via direct measurement of the position. An alternative approach would be to conduct a calibration step where the magnetic field contribution of each magnet is measured at each position within an array of positions that the magnet traverses through. Then, this is used to construct a different $\mathbf{P}$ matrix for each combination of magnet positions from the arrays of each magnet. This second method does not require an accurate model for the magnetic field distribution and does not require knowledge of the magnet absolute locations. Only an accurate indicator, such as a sequence number, that a magnet is in the same position at which the $\mathbf{P}$ matrix was calibrated is required. By obtaining calibration data at each point within an array of potential magnet locations, this sequence calibration method removes the non-linear particle position and orientation information from the problem by creating a magnetic field map of only the relevant portions of each magnet.

For the sequence calibration, the sensors are first placed and baseline calibration data is taken in order to remove the effect of external magnetic fields, such as the magnetic field of the earth. Next, magnet j is added at the desired sensing location and the

magnetic field is recorded for each position with a sequence number k_j such that,

$$P_{ijx}(k_j) = B_{ix}(k_j) - C_{ix}, \tag{15}$$

$$P_{ijy}(k_j) = B_{iy}(k_j) - C_{iy}, \tag{16}$$

$$P_{ijz}(k_j) = B_{iz}(k_j) - C_{iz}. \tag{17}$$

Each subsequent magnet is placed int the system and the magnetic field is recorded for each sequence number. Every magnet can have a different total number of sequence positions and all calibrations should be completed at the same temperature. There are also alternative methods to obtaining the sequence calibrations for different positions. For example, all the magnets can be placed into the system and each magnet can be moved independently to their respective sequence positions. Calibrations can be conducted as long as it is possible to determine the independent contributions of each magnet at each sequence position. Finally, during the experiment, the sequence number for each magnet is recorded and used to construct a different **P** matrix on-the-fly for each data point where the positions of the magnets are different.

EXPERIMENTAL SETUP

The hardware for the system consists of an array of custom magnetic sensor boards, a power supply, a data acquisition card, micrometer stages, reference thermocouples and a personal computer. Figure 3 shows a typical setup for a temperature experiment. The custom magnetic sensor boards utilized Honeywell HMC1053 sensors capable of measuring magnetic fields up to ± 6 G with a resolution of 120 μG. Each of the three axes of the sensor utilizes a Wheatstone bridge to measure the change in magnetoresistance of a thin film of nickel-iron (permalloy) deposited on silicon. The sensors have a low capacitance and therefore have a bandwidth greater than 5 MHz. The permalloy sensors have a temperature coefficient of -0.27 %/°C which is higher than most permanent magnets. Therefore, the sensors either need to be thermally isolated or the chip temperatures have to be monitored and compensated. The high temperature coefficient of permalloy implies that it may be a good choice for future work using paramagnetic particles instead of permanent magnets for temperature sensing.

The sensor boards contain circuitry for a set/reset strap. This utilizes a spiral of metalization on the sensor die for conditioning the magnetic domains in the permalloy during calibration in order to set the polarity of measurements and improve signal linearity. Each sensor board is also coated to protect it from humidity effects. Up to 13 sensors can be hooked up using twisted-pair cable to a custom board that provides a 5 V supply voltage and interfaces with a 16-bit PXI-6255 data acquisition card and a NI-PXIe-1073 chassis with differential analog measurement channels.

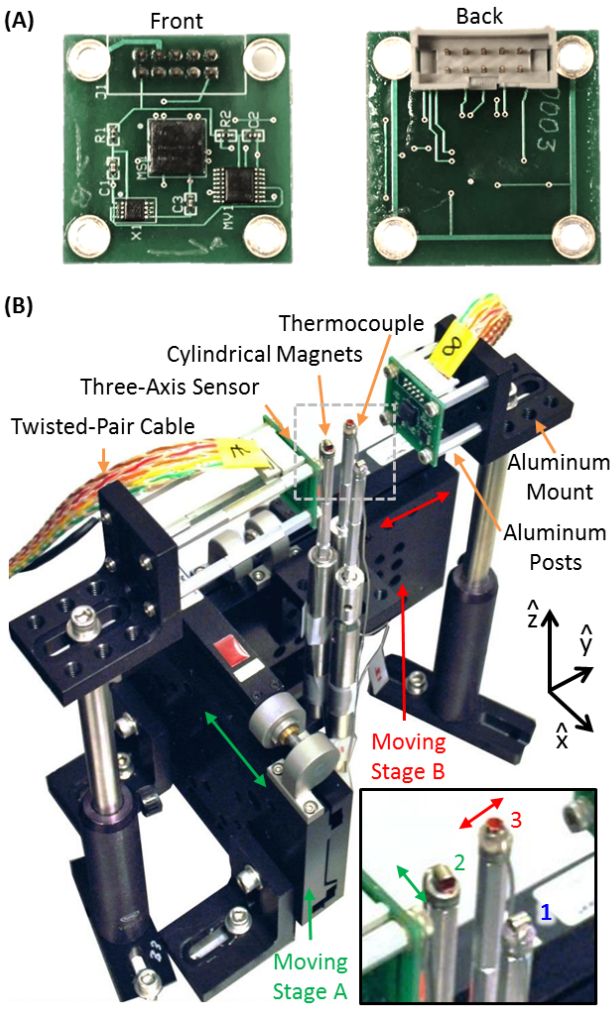

FIGURE 3. (A) THE THREE-AXIS MAGNETIC SENSORS ARE SHOWN ALONG WITH (B) A TYPICAL EXPERIMENTAL SETUP INDICATING THE ARRANGEMENT OF TWO SENSORS, THREE MAGNETS, AND TWO MOVING STAGES. THE INSET SHOWS A CLOSE-UP OF THE THREE MAGNETS AND THE DIRECTIONS OF MOVEMENT FOR MAGNETS 2 AND 3.

Each magnetic sensor board was calibrated using a NIST traceable F. W. Bell 5180 Hall effect gaussmeter and a Helmholtz coil to generate a known, uniform external magnetic field. The sensitivity of each sensor axes was found to be approximately 1 mV/V/G. When the NI DAQ card measurement voltage range is set to $\pm$ 0.1 V, the resolution of the card is 3 μV or 600 μG. The measured standard deviation of the magnetic field signals is generally less than ± 1 mG. User interface software was written in LabVIEW and the program is capable of acquiring data, visualizing the location of the sensors, performing coordinate rotations on the sensor signals, implementing sensor resets and conducting Helmholtz coil calibrations.

Type K thermocouples and a thermocouple acquisition module (NI 9213) were also used to verify and calibrate temperature measurements. These thermocouples contain nickel and have a Curie temperature of 185 °C. They are slightly magnetic, but this effect was compensated for during calibration. Thermocouples are attached to the magnets using a cyanoacrylate adhesive. A variety of temperature sources were used for experiments including hot and ice water as well as a chiller for calibration (Thermo NESLAB RTE 7), which was put in contact with the magnets via thermally conductive copper pipe. Two linear motion stages (CMA-25CCCL) and a motion controller (Newport ESP301-3G) were used to move the magnets in repeatable motions. LabVIEW programs were also used to read the thermocouple measurements, control the chiller, and scan the motion stage.

The mechanical setup uses 24.5 mm spacing optical table components to accurately place magnets and sensors. Plastic screws, aluminum screws, aluminum posts, and anodized aluminum optical bench parts were utilized in the setup to minimize the effects of ferromagnetic and paramagnetic materials. Cylindrical, axially magnetized, nickel-plated N52 grade Nd-Fe-B magnets with a diameter and length of 3.175 mm (K&J Magnetics D22-N52) were used for these experiments.

RESULTS

Magnet Characterization

A magnet has a variety of physical temperature characteristics including its dynamic response, temperature coefficient and non-linear effects and each of these are assessed. The temperature coefficient of the Nd-Fe-B magnets are first calibrated and the magnetic field measurements along the axis of magnetization are shown for the temperature range of 7 to 50 °C in Fig. 4. The sensor is placed approximately 24 mm from the magnet and the magnet is attached to a copper coil, which is temperature controlled using the chiller. One thermocouple is placed on the magnet, another is placed on the coil near the magnet, and the assembly is thermally isolated. The measured temperatures of the two thermocouples are averaged to minimize the biases associated with thermal contact resistance and temperature gradients in the magnet. The magnetic field is monitored and the magnetic field change was measured in Fig. 4 to be approximately $C_T = -0.092\ \%/°\text{C}$. Across seven experiments, the average measured temperature coefficient was found to be $C_T = -0.0912 \pm 0.0031\ \%/°\text{C}$. The temperature coefficient did not vary significantly across the different Nd-Fe-B magnet grades (N35, N48, and N52) tested. In Fig. 4, there is a slight amount of reversible hysteresis, which may cause temperature estimation errors of approximately $\pm 2°\text{C}$ if it is not modeled. Above approximately 60 °C for these magnets, irreversible hysteretic temperature behavior occurs. Different magnet grades can be used if higher operating temperatures are desired.

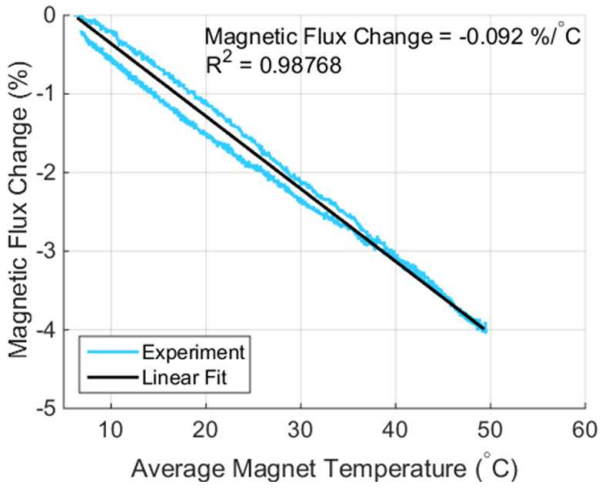

FIGURE 4. THE RELATIONSHIP BETWEEN MAGNETIC FIELD CHANGE AND TEMPERATURE IS SHOWN FOR A NEODYMIUM IRON BORON MAGNET.

For cylindrical magnets with a diameter and length of 3.175 mm, the thermal time constant for a fully immersed (surrounded on all sides by hot water) magnet is 1.91 ± 0.23 s. If only the top, circular face of the magnet is exposed, the time constant becomes longer, on the order of 11.5 s, since less area is exposed. If faster time constants are required, smaller magnets can be used or more area can be exposed to the temperature source. Alternatively, system identification techniques can be used to determine the thermal impulse response to estimate the instantaneous applied temperature via deconvolution.

Stationary Magnet Temperatures

In many applications, such as inside batteries, the magnets and sensors can be stationary and a single **P** matrix can be obtained from the calibrations. Figure 5 shows the measured magnetic field on two sensors for three different stationary magnets with thermocouples attached in the configuration shown in Fig. 3(B) and listed in Table 1. Because the stage translation was slow, the sampling rate was limited 0.28 Hz to allow time for the stage positions to settle.

Each thermocouple and magnet is wrapped in Teflon tape (such that only one face of the magnet is exposed) to isolate each assembly from the effect of external temperature sources that may come in contact with the thermocouples and not the magnets. For this experiment, cold ice-water is applied to each magnet in sequence. Then hot water is applied using a squeeze bottle to each magnet in sequence. Because the magnets are stationary in this experiment, the magnetic field does not change significantly over time but the small changes in magnetic field magnitudes due to temperature changes can be seen, especially

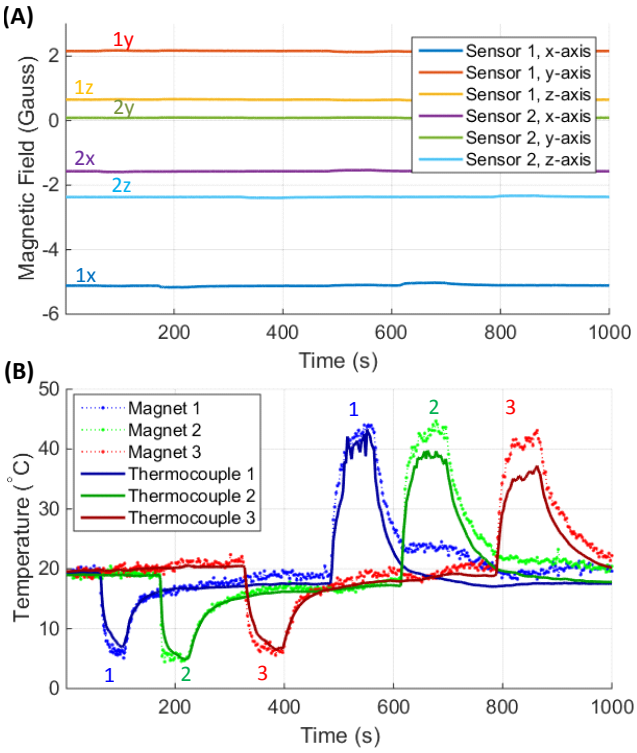

FIGURE 5. (A) THE MAGNETIC FIELD OF TWO THREE-AXIS SENSORS AND THREE MAGNETS IN A STATIONARY CONFIGURATION IS SHOWN ALONG WITH (B) THE TEMPERATURE ESTIMATES FROM MAGNETIC FIELD INVERSION FOR THE THREE MAGNETS. REFERENCE THERMOCOUPLE MEASUREMENTS ARE ALSO SHOWN.

for the x-axis of Sensor 1 in Fig. 5(A). It is also clear that it would be difficult to manually determine the temperature of each magnet by simply looking at the magnetic field values.

From Fig. 5(B), it is clear that the matrix inversion solutions for the temperatures of each magnet matches well with the results from the thermocouples attached to each magnet. From this experiment, the temperature time constant when only one face of the magnet was exposed was measured to be approximately 10 seconds, which is close to the time constant estimate made earlier. Because there is some residual thermal contact resistance between the magnet and the thermocouple, the thermocouple measurements have a smaller temperature change than the magnet measurements. In addition, because the magnet size is significant, one side of the magnet may be at a different temperature than the side of the magnet where the thermocouple is attached. Therefore, some temperature changes from radiative or convective heat transfer that are measured by the average magnetic field temperature estimates may not show up on the thermocouple measurements. In this experiment, the temperature estimation noise has a standard deviation of approximately 0.45 °C. These results clearly show that it is possible to decouple the magnetic field contributions from three closely-spaced magnets and obtain an accurate estimate of their temperatures independently.

TABLE 1. APPROXIMATE MAGNET AND SENSOR POSITIONS AND ORIENTATIONS IN THE GLOBAL COORDINATE FRAME

	Position			Orientation		
	a (mm)	b (mm)	c (mm)	m	n	p
Magnet 1	-2.5	-7.0	-5.0	-0.97	-0.24	0
Magnet 2	-7.5	8.0	-2.0	0.45	0.89	0
Magnet 3	7.5	9.0	1.0	0	0	-1
	Position					
	x (mm)	y (mm)	z (mm)			
Sensor 1	27.5	0	0			
Sensor 2	-27.5	0	0			

Moving Magnet Temperatures

For applications with moving components, a **P** matrix must be constructed for each time step where the position of at least one magnet changes. Figures 6 and 7 show an experiment with two sensors and three magnets where two of the magnets are translated. The same temperature application procedure, magnet starting points, and magnet orientations were used in this experiment as in the earlier stationary experiment. In this experiment, magnet 2 is translated by 12 mm back and forth in the positive y direction and magnet 3 is translated by 6 mm back and forth in the positive x direction in 0.2 mm step size increments. The position change is shown in Fig. 6(B).

Only one calibration for magnet 2 from positions 0 to 12 mm (61 total points) and one calibration for magnet 3 from positions 0 to 6 mm (31 total points) was obtained. During the experiment, no two time steps have the same position for magnet 2 and magnet 3. This is indicated in Fig. 6(B) where the position changes in magnet 2 and magnet 3 are slightly out of phase. This clearly shows how it is possible to obtain a large number of different **P** matrices (244 different matrices, one for each position combination of the two moving magnets) from shorter calibrations.

In Fig. 6(C), it is clear that the magnetic field values change significantly and it is difficult to distinguish temperature changes on each magnet by eye because the position changes causes a much larger variation in the magnetic field than the temperature. In Fig. 6(D), the same **P** matrix is used for the entire experiment to illustrate the difference between the sensitivities for position and temperature. It is clear that the temperature estimates are poor with errors as large as 1000 °C if translations up to 6 mm are not accounted for. However, if different **P** matrices are used to account for the position changes in magnets 2 and 3, then the temperature estimates in Fig. 7(A) are obtained. It is clear that

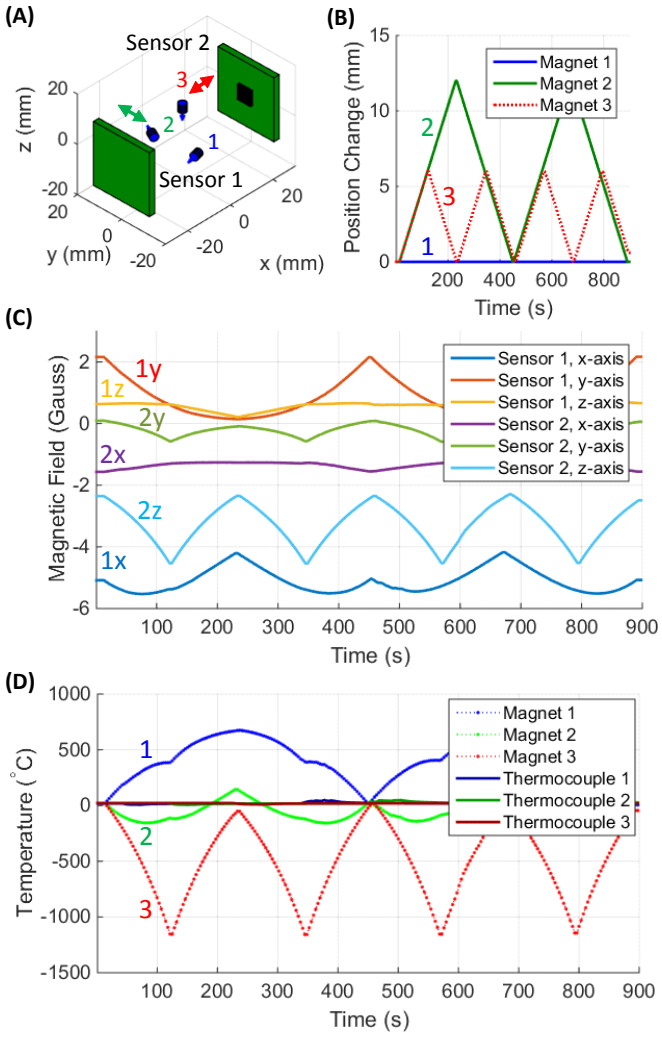

FIGURE 6. (A) MAGNET 2 AND 3 ARE MOVED IN THE DIRECTIONS INDICATED AND (B) THEIR CHANGE IN POSITIONS OVER TIME ARE SHOWN. (C) THE MAGNETIC FIELDS ARE PLOTTED ALONG WITH (D) THE ESTIMATED TEMPERATURES WHEN THE SAME $\mathbf{P}$ MATRIX IS USED FOR THE ENTIRE EXPERIMENT SOLUTION. THIS IS USED TO SHOW THAT THE SENSITIVITY TO POSITION IS MUCH GREATER THAN THE SENSITIVITY TO TEMPERATURE.

once the position changes are accounted for, the temperature estimates can be recovered accurately and there appears to be no residual effects from magnet motion.

Figure 7(B) shows all the condition numbers for the $\mathbf{P}^T\mathbf{P}$ matrices used for the temperature solutions in the experiment. The condition number is the ratio of the largest and smallest singular value of a matrix [13]. From this plot it is clear that some magnet position combinations introduce more sensitivity than other combinations, but the matrix condition number is generally good. The closer the magnets and sensors are to each other (without saturating the sensor), the higher the temperature sensitivity

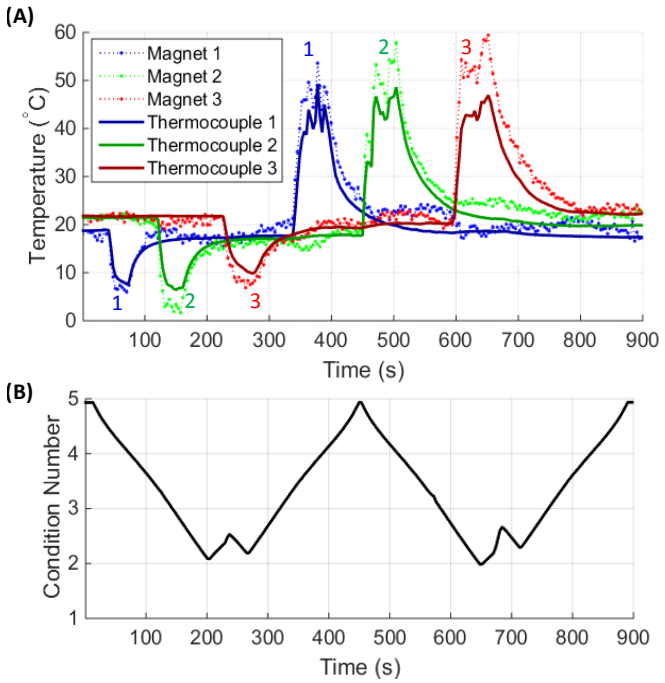

FIGURE 7. (A) WHEN A DIFFERENT $\mathbf{P}$ MATRICES ARE USED TO COMPENSATE FOR POSITION CHANGES IN THE EXPERIMENT DETAILED IN FIG. 6, THEN IT IS POSSIBLE TO ACCURATELY RECOVER THE TEMPERATURE AT EACH MAGNET. (B) THE CONDITION NUMBER FOR EACH $\mathbf{P}^T\mathbf{P}$ MATRIX IS ALSO SHOWN.

and the lower the noise levels. Due to the sensor bit-depth, electronic and magnetic field noise, and size of the magnets (which influences the magnetic field magnitude) chosen for this experiment, the range of motion for a low-noise temperature measurement is limited to be between 10 and 30 mm from the nearest sensor. Additional sensors, higher range sensors or higher sensitivity magnetic field sensor systems can be used to extend the range of motion.

Movement of Metal Components

Conventionally, magnetic particle tracking cannot be done in the presence of ferritic materials or materials which bend the magnetic field. Using the calibration procedures presented in this work, however, it is possible to sense temperature in the presence of metals if these materials are tracked and move in repeatable motions. Table 2 shows how materials with different permeabilities can affect the magnetic field signal. In these experiments, a z oriented magnet is placed 32 mm from a sensor and the magnetic field is measured. A large 152 $\times$ 152 mm metal sheet that is 1.2 to 1.3 mm thick is moved back and forth between the sensor and the magnet. The magnetic field deviation in the z axis near the center of the plate as a percentage of measured field with no metal plate is presented in the third column.

TABLE 2. THE MAGNETIC FIELD DEVIATION IN THE PRESENCE OF METAL PLATES AND THE MEASUREMENT REPEATABILITY AS A FUNCTION OF MOVEMENT OF THE METAL PLATE ON A STAGE

Material	μ_r Ref. [14]	Field Deviation (%)	Repeatability (G)
Air	1	0.06 ± 0.04	0.10 ± 0.08
Copper	1	0.06 ± 0.05	0.15 ± 0.09
Aluminum 6061	1	0.06 ± 0.04	0.15 ± 0.13
Stainless 304 (Austenitic)	1 to 7	0.50 ± 0.52	0.14 ± 0.12
Stainless 313 (Austenitic)	1 to 7	0.54 ± 0.37	0.11 ± 0.09
Stainless 410 (Martensitic)	95 to 750	34.0 ± 3.48	0.14 ± 0.10
Stainless 430 (Ferritic)	1800	86.6 ± 4.90	0.16 ± 0.10

For these experiments, 1.2 to 1.3 mm thick metal plates are moved back and forth between a z oriented magnet and sensor placed 32 mm apart.

Materials like copper and aluminum have a relative permeability near unity and therefore do not alter the field magnitude at all. Austenitic stainless steels can have a relative permeability near unity or slightly higher, especially if they are cold worked. Since these materials are cut with sheet metal break, the edges of the stainless steel will have a higher relative permeability leading to the slightly larger measured field deviations. Martensitic and ferritic stainless steels will have even higher relative permeabilities and will alter the measured field significantly. These materials also tend to be much less uniform and the relative permeability changes significantly as a function of position and orientation of the metal sheet. In some samples and orientations, the deviation observed in the martensitic material can exceed the deviations measured from the ferritic material. If the movement of these metal components is not tracked, then the field deviations listed in the table represent the magnetic field error that can be expected and Eqs. (2)-(4) and Eq. (14) can be used to calculate the expected temperature error. However, if the motions of these metals are tracked and calibrated accurately, then these errors can be removed from the temperature estimate.

In the last column, the repeatability of the magnetic field measurements is measured as the metal sheets are inserted and withdrawn from the magnet and sensor setup. The metal sheets are attached to a slow stage traversing up to 20 mm in 0.5 mm intervals. Before the sheet was inserted, the maximum distance between the sheet edge and the magnet-to-sensor centerline was 13 mm for each sample. The field near the edges of the metal is measured, instead of near the center, because this creates the greatest change in magnetic field as a function of position. The magnetic field at each position is measured multiple times and the repeatability is reported. Although the ferritic stainless steel causes large deviations in the measured field magnitude, the repeatability of the signal through multiple passes is approximately the same as for all the other materials. Therefore, the magnetic field repeatability is essentially only a function of stage positioning repeatability and inherent sensor electrical noise, and not a function of material permeability. This shows that as long as the movement of the material is repeatable and tracked, the temperature sensing scheme can be applied in the presence of metals, including ferritic metals.

Due to the change in the field magnitude, however, the temperature estimation noise for the configuration with ferritic metals may increase. This is because the temperature estimate, for the example of a single magnet and single sensor axis, is essentially the change in the field due to temperature divided by the magnitude of the field without temperature changes. Therefore, if the magnitude of the field decreases and the noise level (or repeatability) is fixed, then the temperature measurement error must increase. Depending on the configuration, magnetic field contributions from materials with $\mu_r \neq 1$ may not sum linearly with existing magnetic fields. Therefore, sequence number calibrations should be conducted for each permutation of interest for the positions of the $\mu_r \neq 1$ metal and magnets.

CONCLUSIONS

Previous work by other groups use three-axis magnetic field sensors mostly for magnetic particle tracking applications [8]. Because the change in magnetic field due to temperature is much smaller than the change in the field due to movement, there has been little emphasis on temperature sensing with magnets. Some prior art on temperature measurements use only a single magnet at a fixed distance from a sensor [2, 5, 7]. The techniques proposed in this paper are able to measure the temperature of multiple magnets while the magnets are stationary or undergoing repeatable motions using least squares inversion. The instrumentation, limitations, and calibration procedures for the experiment are discussed and the results show that it is possible to track the temperature of multiple stationary or moving magnets.

The use of permanent magnets for measurements can have a few drawbacks. Untracked or unknown movement of objects in the system that can generate or alter magnetic fields can potentially cause errors in the temperature estimation. This can include the movement of untracked ferromagnetic materials such as ball bearings or the untracked changes in electric fields from DC motors. For the experiments in this paper, which contains both ball bearings and DC motors, no magnetic field disturbance was observed for the distances we used. In general, however, the distance between the temperature sensing system and unpredictable magnetic field generating or altering components should made as large as possible. Magnetic field shielding can also be used. If the magnitude of the magnetic field disturbances from these ferromagnetic, paramagnetic or electric-field generating objects can be quantified, Eq. (14) can be used to predict the temperature estimation error due to these objects in order to determine the minimum acceptable distances for a given application and set of components.

On the other hand, if field generating or altering components are stationary or move in known repeatable motions, it is possible to conduct accurate temperature sensing near these component. By using a modified version of the sequence number calibration procedure presented in this work on each paramagnetic or ferromagnetic component, it is possible to minimize the temperature estimation error from these magnetic field disturbances. The sensing procedure presented here would also work near dynamic electric fields if the electric fields changes are repeatable and can be indexed. In general, materials with permeability near unity, including 304, 313 and 316 stainless steel, can be used near this sensing system without the need for additional sequence number calibrations.

There are many possible extensions to this work including measuring the temperature of a large distribution of magnets in order to determine the source of a hot spot. Optimal magnet and sensor placement analysis would also be useful for minimizing the error and improving the least squares inversion. In addition, it would also be important to understand how adding or removing sensors can affect the noise in the estimate for each magnet. Measuring position, orientation, and temperature of a magnet simultaneously would also be an interesting area of future work. The concepts proposed in this paper present a unique sensing capability for the wireless measurement of multiple temperature points moving in a repeatable fashion and can be used on robotic manipulators, for automation systems, and inside opaque enclosed vessels.

ACKNOWLEDGMENT

The authors would like to thank Amanda Dodd, Emily K. Stirrup, Stephen S. Miller, Harriet Li, and Joseph Buttacci for their previous work and assistance with the project. This work was supported by the Laboratory Directed Research and Development program.

REFERENCES

[1] Kovacs, A., Peroulis, D., and Sadeghi, F., 2007. "Early-warning wireless telemeter for harsh-environment bearings". In Proceedings of the 2007 IEEE Sensors Conference, pp. 946–949.

[2] Gupta, L. A., and Peroulis, D., 2013. "Wireless temperature sensor for condition monitoring of bearings operating through thick metal plates". *IEEE Sensors Journal,* ***13***(6), pp. 2292–2298.

[3] Gupta, L. A., Young, L., Wondimu, B., and Peroulis, D., 2013. "Wireless temperature sensor for mechanical face seals using permanent magnets". *Sensors and Actuators A,* ***203***, pp. 369–372.

[4] Fletcher, R. R., and Gershenfeld, N. A., 2000. "Remotely interrogated temperature sensors based on magnetic materials". *IEEE Transactions on Magnetics,* ***36***(5), pp. 2794–2795.

[5] Mavrudieva, D., Voyant, J.-Y., Kedous-Lebouc, A., and Yonnet, J.-P., 2008. "Magnetic structures for contactless temperature sensor". *Sensors and Actuators A,* ***142***, pp. 464–467.

[6] Fletcher, R., and Gershenfeld, N., 2001. Wireless monitoring of temperature. US Patent 6,208,253 B1.

[7] Gupta, L. A., and Peroulis, D., 2012. "Wireless temperature sensor operating in complete metallic environment using permanent magnets". *IEEE Transactions on Magnetics,* ***48***(11), pp. 4413–4416.

[8] Yang, W., Hu, C., Li, M., Meng, M. Q.-H., and Song, S., 2010. "A new tracking system for three magnetic objectives". *IEEE Transactions on Magnetics,* ***46***(12), pp. 4023–4029.

[9] Lee, K.-M., and Son, H., 2007. "Distributed multipole model for design of permanent-magnet-based actuators". *IEEE Transactions on Magnetics,* ***43***(10), pp. 3904–3913.

[10] Wu, F., Frey, D. D., and Foong, S., 2013. "A hybrid magnetic field model for axisymmetric magnets". In Proceedings of the 2013 IEEE/ASME International Conference on Advanced Intelligent Mechatronics, pp. 786–791.

[11] Foong, S., Lee, K.-M., and Bai, K., 2012. "Harnessing embedded magnetic field for angular sensing with nanodegree accuracy". *IEEE/ASME Transactions on Mechatronics,* ***17***(4), pp. 687–696.

[12] Hu, C., Meng, M. Q.-H., and Mandal, M., 2006. "The calibration of 3-axis magnetic sensor array system for tracking wireless capsule endoscope". In Proceedings of the 2006 IEEE/RSJ International Conference on Intelligent Robots and Systems, pp. 162–167.

[13] Rynne, B. P., and Youngson, M. A., 2008. *Linear Functional Analysis*, 2nd ed. London: Springer.

[14] Carpenter Technology Corporation, 2016. Magnetic properties of stainless steels. [Online]. Available: http://www.cartech.com/techarticles.aspx?id=1476.